

EXPERIMENTAL PLATFORM FOR CHARACTERIZING A NYLON THREAD THERMOMECHANICAL ACTUATOR

KARLA ALMEIDA*, SAULO LUIZ†, ANTÔNIO M.N. LIMA†, JOÃO ARAÚJO*

**Post-Graduate Program in Electrical Engineering - PPgEE - COPELE*

†*Electrical Engineering Department (DEE)
Federal University of Campina Grande (UFCG)
58429-900, Campina Grande - PB - Brazil*

Emails: karla.almeida@ee.ufcg.edu.br, saulo@dee.ufcg.edu.br, amnlima@dee.ufcg.edu.br, joao.araujo@ee.ufcg.edu.br

Abstract— The present work has as objective to develop and execute the project of an experimental platform to obtain the electro thermomechanical responses of a class of actuators based on nylon fishing lines. The methodologies used for the hardware and software development were the Model-Based Design, automatic code generation, and the V Model methodology. The tests for validating the platform demonstrated a capacity of a 120 mm in length and 1 mm diameter actuator perform work and lift a load of 150 g, contracting up to 15.2 mm (12.67%), and to generate a force of up to 2.36 N, when submitted to a temperature of 156.4 °C in response to an input signal of electric current of average value of 6.6 A controlled by PWM that flowed through a 0.8 mm diameter copper wire wrapped on the actuator.

Keywords— actuator, nylon, characterization, Model Based Design.

1 Introduction

Haines et al. (2014) reported an important phenomenon of practical application: if a monofilament nylon fishing line (MNFL) is subjected to a torsion process under tension, and acquires a spring shape, then it may be used in actuators for generating repetitive and reversible contractions under heating/cooling cycles. This phenomenon motivates a promising alternative in relation to the shape memory alloys (SMA). The SMAs typically exhibit non-linearities, hysteresis and linear displacement capacity of 4 to 5%, according to Seelecke and Muller (2004). The MNFL exhibit linear behavior, low hysteresis and linear displacement capacity of the order of 20%, according to Haines et al. (2014). Furthermore, the manufacturing process is simple and inexpensive. However, it has a limitation: nylon monofilament does not conduct electric current, so to heat it by means of the Joule effect, as is commonly done with shape memory alloys, it is necessary to provide a heating structure, such as a wrapped conductive wire to the actuator, for example.

According to Mirvakili et al. (2014), the actuation mechanism presented by Haines et al. (2014) suggests that the torsion process reorients the polymeric chains of the nylon in a helicoidal manner, decreasing the length and increasing the diameter of the fibers. During the heating, these helicoidal chains suffer an anisotropic thermal expansion which produces an axial contraction and at the same time a linear expansion, inducing a distortion of the fiber. As the thread is coiled, this reversible twisting is converted to a linear movement, triggering the actuator's contraction.

This type of linear actuator has been the sub-

ject of considerable interest on the part of the academy, due to its elastic similarity with human muscles as demonstrated by Yip and Niemeyer (2015) and wide range of operation in temperature, functional for automotive and aerospace applications as demonstrated by Kianzad et al. (2015). Although this technology is promising, it is still in its early development phase. In this context, this work had, as objective, developing and executing the project of an experimental platform to characterize the behavior of a nylon actuator triggered by the Joule effect.

The experimental platform design was based on the Model-Based Design methodology proposed in Aarenstrup (2015), automatic code generation, and the V-Model approach for hardware and software development. These methodologies were chosen because they require verification and validation tests at all stages of the project, reducing the risks of failures and ensuring correctness. In addition, aiming at a later phase of modeling and control, the software was developed by means of the blocks diagrams in simulation environment, verification and automatic code generation for hardware.

Some platforms have been presented in the literature with different characteristics and purposes. The one developed in this work has important functionalities to study the dynamic behavior of nylon actuators. One of them is the control and measurement of the input, an electric current, in contrast to the works of Yip and Niemeyer (2015), Sutton et al. (2016) and Arakawa et al. (2016) that use the electric voltage as the system input. By means of the platform developed in this work it is also possible to perform isotonic and isometric tests in the same structure, in counterpart to those

developed by Moretti et al. (2015) and Cho et al. (2016).

The remaining of this text is organized as follows. In Section 2, we present the theoretical model of the nylon actuator, which is the basis for the definition of the system requirements. In Section 3, we present the stages of the platform design and the methodology of the experiments. In Section 4, are presented the results of the actuator electro thermomechanical characterization. The conclusions of this work are presented in Section 5.

2 Actuator model

Yip and Niemeyer (2015) and Sutton et al. (2016) have shown that the force exerted by a nylon actuator may be modeled by a mass-spring-damping system with a linear term dependent on the temperature. This system is represented in Figure 1, where m is the mass of a load, x_0 is the length of the actuator without the load, x_1 is the actuator's length with the load in equilibrium, x is the displacement of the actuator when heated, k is the elasticity coefficient of the spring [N/m], b is the damping coefficient [N/m·s], p is the thermal constant [N/°C], T is the actuator temperature and T_a is the room temperature.

2.1 Thermomechanical model

The thermomechanical model may then be represented by the differential equation in (1). The temperature dependent term, F_T , is given by (2).

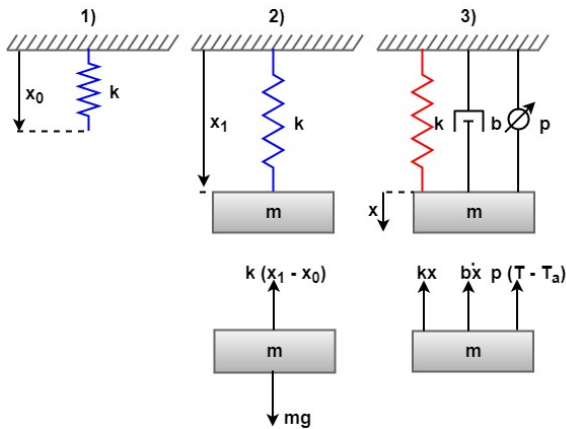


Figure 1: Free body diagram.

$$m\ddot{x} = -kx - b\dot{x} - p(T - T_a) \quad (1)$$

$$F_T = p(T - T_a) \quad (2)$$

In part 1 [see Figure 1-1], the actuator is at its initial length and free of forces. In part 2 [see Figure 1-2] a load is hung at the actuator's end, increasing its length from x_0 to x_1 and the load's weight is balanced by the elastic force. In part 3

[see Figure 1-3] a force due to the temperature rising displaces the actuator (implying the existence of an elastic force related with the displacement x), and a viscous friction force due to speed \dot{x} . As the nylon actuator contracts due to the temperature increase, the displacement x is typically negative. Thus, the model given by (1)-(2) may also be described by

$$\frac{X(s)}{F_T(s)} = -\frac{\frac{1}{m}}{s^2 + \frac{b}{m}s + \frac{k}{m}} \quad (3)$$

In the next section, we present the relationship between the force F_T and the electric signal by which the actuator's temperature $T(t)$ is changed will be discussed.

2.2 Thermoelectric model

The nylon actuator is triggered thermally. Thus it may be heated by means of the Joule effect caused by a flowing through which surrounds the actuator, as shown in Figure 2.

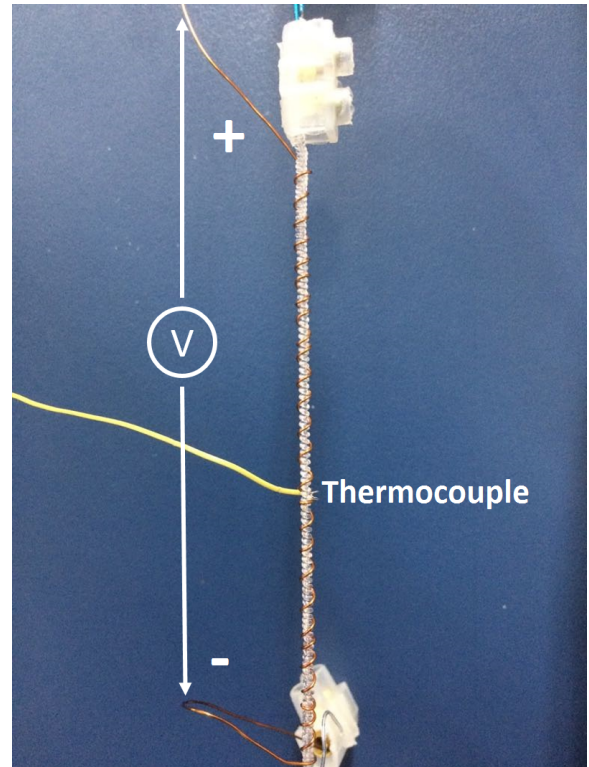


Figure 2: Heating the actuator by means of the Joule effect.

In this context, considering the basic concepts of thermodynamics, energy conservation, and heat transfer, the thermoelectrical model may be expressed by the equation of thermal equilibrium of heat transfer presented in (4), where C is the actuator's thermal capacity [J/°C], I^2R is the power from Joule effect [W], and G is the actuator absolute thermal conductivity [J/°C·s] at room temperature [T_a].

$$C\dot{T} = I^2R - G(T - T_a) \quad (4)$$

The electrical resistance of a wire conductor varies with the temperature, according to (5), where R_0 represents the wire resistance [Ω] at room temperature T_a and α is the wire temperature coefficient [$^{\circ}\text{C}^{-1}$]

$$R = R_0[1 + \alpha(T - T_a)] \quad (5)$$

Based on (2), (4) e (5), the thermoelectrical model presented in (6).

$$\dot{F}_T = f(F_T, I) = \left(\frac{pR_0}{C} + \frac{R_0\alpha}{C}F_T\right)I^2 - \frac{G}{C}F_T \quad (6)$$

2.3 Electro-thermo-mechanical model

The nylon actuator electro-thermo-mechanical model is represented by the block diagram in Figure 3, where the relations between the thermo-mechanical and thermoelectrical subsystems are presented. In this model, the system input is the electric current, and the output is the actuator displacement.

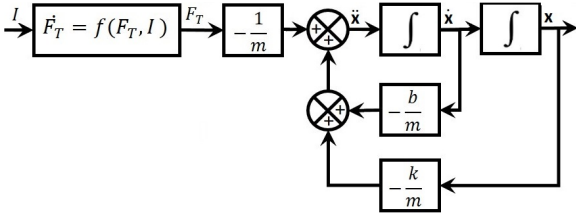


Figure 3: Block diagram of the nylon actuator model.

3 Materials and Methods

The design phases of the project are represented in Figure 4 and are detailed in the following sections.

3.1 High-Level Specifications

The electro thermomechanical characterization of the the third order thermomechanical model, and the position control of the nylon actuator must all be performed by means of a single experimental test platform. Thus, such plataform must be composed of: sensors for measuring the position, the force exerted by, and the temperature of the nylon actuator, along with the current flowing through the wire which surrounds the actuator; and a drive circuit for such current.

The acquisition and data processing of the sensors and the control signals for the actuators must be performed by means of a microcontroller. The software for the microcontroller may be developed by means of block diagrams, from which the code may be automatically generated.

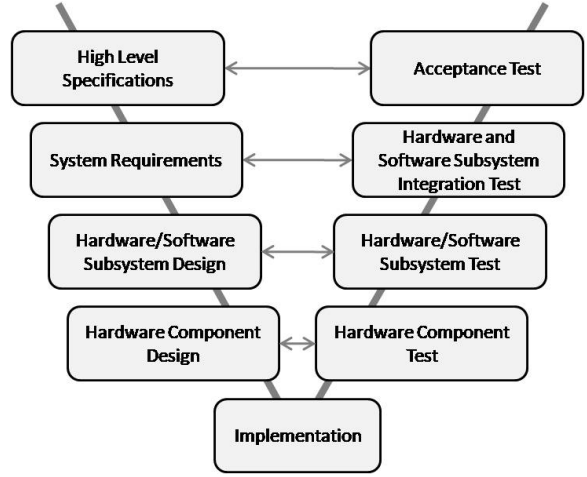


Figure 4: Steps of the V-Model methodology. Own authorship.

3.2 System requirements

To fulfill the high-level specifications presented in Section 3.1, it is necessary to find the ratios of inputs and outputs of the system, according to the equations presented in Section 2. The experiment consists of heating and cooling the actuator by means of electric current flowing through a conducting wire; and measuring the output signals: temperature, pulling force and displacement.

The requirements that the platform must meet have been defined through preliminary experiments to identify the operating limits of the actuator, and these are the following: apply and measure an electric current of up to 7 A, measure a temperature between 25 $^{\circ}\text{C}$ and 160 $^{\circ}\text{C}$, measure the exerted traction force, of up to 2.5 N, and measure displacement of up to 15 mm caused by the actuator contraction.

3.3 Hardware subsystem design

In this section, the requirements and design of the hardware units and subsystems will be presented. For each project, simulations were conducted in a simulation software of electronic circuits and the components specifications were determined as a function of the obtained results.

Electrothermal Triggering

This subsystem function is to inject an electric current of up to 7 A, controlled by a pulse width modulated (PWM) signal, in a 0.8 mm diameter copper wire which surrounds the actuator, and a circuit to measure such current.

In order to meet these specifications, a circuit was designed for controlling PWM signal, which is applied to a MOSFET IRFZ46N transistor, which works as an ON/OFF switch between a 3 V power source and the copper wire.

An electric circuit was designed for measuring the electric current. Such circuit is composed

of a Shunt resistor of 13 m Ω , whose characteristic curve will be presented in Section 3.6. Such shunt resistor is connected in series with the 0.8 mm diameter copper wire. As the maximum current is of 7 A, the voltage drop on the Shunt is of up to 104 mV. Therefore, this sensor signal was conditioned by an instrumentation amplifier INA101 and was later applied to a low-pass RC filter to eliminate the PWM's DC component. A gain value of 41 was obtained by connecting an external resistance of 1 k Ω to the INA101 for an output signal of 5 V maximum.

Temperature Measurement

This subsystem's function is to measure the actuator's temperature of up to 160 $^{\circ}\text{C}$ during the electrothermal triggering. A type k microthermocouple whose diameter is 0.3 mm was selected. Such diameter is appropriate for the actuator's diameter of 1 mm.

The microthermocouple output signal is not directly related to the measurement joint temperature, but to the temperature gradient, that is, the difference between the measurement joint temperature and the reference joint temperature. Thus, it is necessary to know the reference joint temperature, which must always be in an isothermal environment. A circuit was designed with the AD595 device, which is an instrumentation amplifier and a cold joint thermocouple compensator on a monolithic chip. It combines an ice point reference with an amplifier pre-calibrated to produce an analogical output of 10 mV/ $^{\circ}\text{C}$ directly from a thermocouple signal. An RC low-pass filter was connected to the AD595's output for eliminating the noise.

Mechanical Force Measurement

This subsystem function is to measure the traction force of up to 2.5 N generated by the actuator due to its heating. The chosen transducer was a strain gauge cell that has a nominal capacity of 5 kg and an analogical output signal of 0 to 24 mV.

This transducer output signal is related to a traction force in kgf. In Section 3.6, we present how the characteristic curve of this transducer was determined. The conversion to N was performed by means of the software (microcontroller programming).

In order to improve the data acquisition by the microcontroller, a circuit was designed with INA-101HP with a 200 Ω gain resistor to amplify the output signal by 200. A RC low-pass filter was connected to attenuate the noise.

Displacement Measurement

This subsystem function is to measure the linear deformity of up to 15 mm caused by the actuator contraction. The selected transducer was an LVDT with a measurement band of -25 mm to 25 mm, output analogical signal band of -5 V to 5 V, and resolution of 0.2 V/mm.

A circuit with the LM324 amplifier was designed for conditioning the transducer output signal to a microcontroller input. Such amplifier was used as a buffer with an offset adjust and a voltage divider, generating an output of 1.75 V to 4.25 V, corresponding to the measurement band of 0 to 50mm. This relation is not linear. The characteristic curve that relates the output signal to the displacement is presented in Section 3.6.

Microcontroller

A microcontroller must be used for the data acquisition, signal generation, and signal processing required by the subsystems presented in the previous sections. The minimum hardware specifications for such microcontroller are four analogic inputs and a PWM output. The AT-MEL ATmega2560 microcontroller on the Arduino Mega2560 board satisfies such. It provides 8 bits PWM outputs and 10 bits resolution analog inputs.

At the microcontroller inputs A0, A2, A4 and A6, the conditioning circuits outputs of the Shunt, thermocouple, load cell and LVDT were connected, respectively. A microcontroller PWM output was connected to the electrothermal drive circuit input. The integration between the hardware subsystems is shown in the block diagram in Figure 5. In the Section 3.5, the software subsystems developed for the microcontroller will be described.

3.4 Testing of hardware units and subsystems

In this step, each component of the subsystem was individually tested on a protoboard aided by a power source, function generator, oscilloscope, and multimeter. Afterwards, the projects were implemented on printed circuit boards, integrating the components. After the hardware integration, the hardware verification was performed.

3.5 Design and simulation of software subsystems

The software subsystems were designed and simulated using block diagrams. It was not necessary to test each component because these are elementary reading blocks of the microcontroller A / D converter and basic math operations.

For each input signal from a hardware subsystem, a block was used for acquiring the signals read by the A/D converter and a block for converting these values for their voltage values. The acquisition blocks were set for the inputs A0, A2, A4 and A6 for the input signals from the Shunt, thermocouple, load cell and LVDT, respectively. The conversion blocks were set in 5/1023. Then, for convert to physical values, the respective characteristics curves of the sensors and the functions were implemented along with the output blocks. The characteristics curves will be presented in the

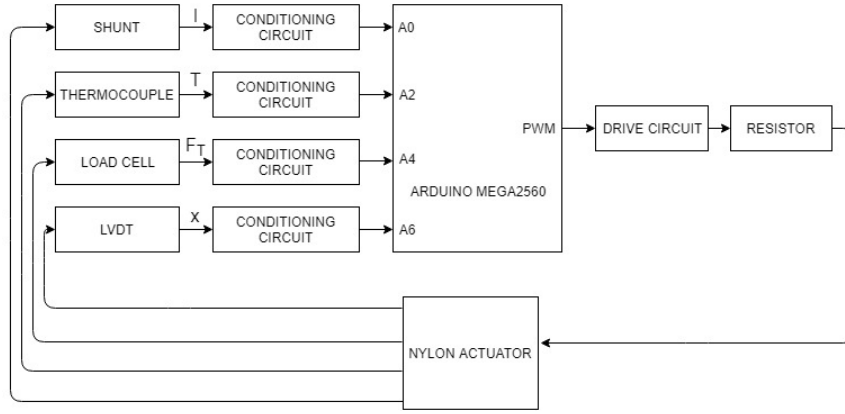


Figure 5: Block diagram of the hardware subsystem.

next section, because it corresponds to the integration hardware and software.

A function generator block and a PWM writing block were used for generating an input current signal controlled by PWM for the actuator's triggering software subsystem. In order to excite the system in different operation points of the actuator, the function generator block was designed for varying the amplitude of the electric current starting from the duty cycle of 10% to 100%, at a steps of 10%.

The software subsystems integration, which is the routine of the dynamic experiment, consisted on selecting and grouping the subsystems: actuator triggering, electric current measurement, temperature measurement, force measurement, and displacement measurement, as show in Figure 6.

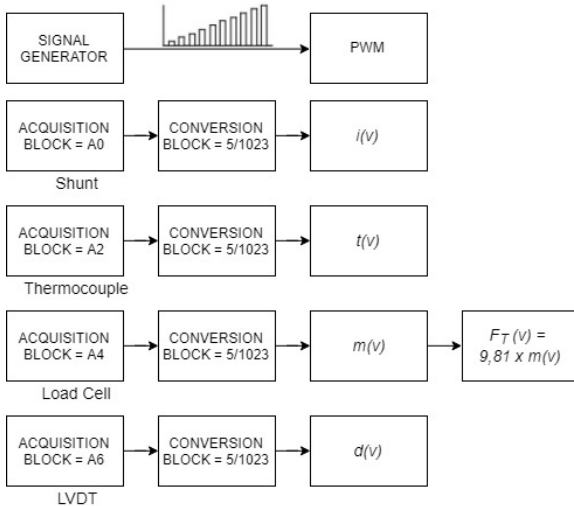


Figure 6: Block diagram of the software subsystem.

3.6 Hardware-software integration

The hardware and software integration of each subsystem was accomplished by automatically generating the code of the software system for the

microcontroller to which the other hardware subsystems were integrated. In this step, the characteristic curve of each sensor was obtained. The procedures are presented in this section.

For the Shunt resistor characterization, the circuit described in Section 3.3 was modified by connecting an amperemeter and a power resistor of 10Ω serially with the Shunt. The power source's voltage was varied from 1 V to 20 V every 10 s, at steps of 1 V, the current and voltage values were read and saved. The curve fitting equation is $i(v) = \frac{1}{13 \times 10^{-3}} v$.

For the load cell characterization, the circuit presented in Section 3.3 was used. The calibrated weights varying from 50 g to 1 kg, at steps of 50 g, were connected to the load cell hook. For each weight, the load cell output signal was read and saved. The characteristic curve found is shown in Figure 7.

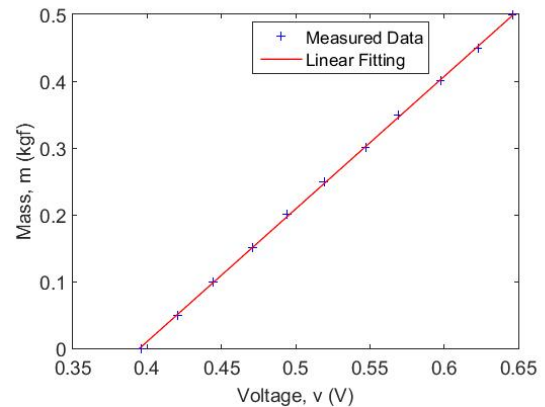


Figure 7: Load cell characteristic curve and the respective curve fitting $m(v) = 1.9v - 0.7745$.

For the LVDT characterization, the circuit presented in Section 3.3 was used. The axis of a step motor was connected by a toothed belt to a pulley's axis that was connected to the LVDT stem, in such a way that one step of the motor corresponded to a linear movement of the LVDT's

stem of 0.25 mm. For each step of the motor, the LVDT's displacement was measured with a vernier caliper and the voltage signal was read by means of the microcontroller. The characteristic curve found is presented in Figure 8.

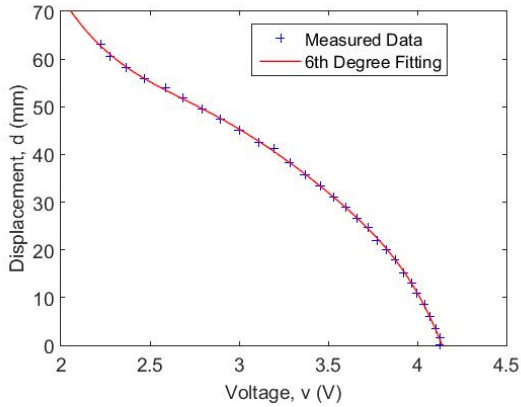


Figure 8: LVDT characteristic curve and the respective curve fitting equation $d(v) = -3.9v^6 + 63.6v^5 - 417v^4 + 1389.8v^3 - 2409.4v^2 + 1918.8v - 352$.

The procedure for obtaining the characteristic curve was not performed for the thermocouple, because the association of the AD595 with the RC filter has a linear output of $10 \text{ mV}/^\circ\text{C}$. Then, the characteristic curve equation is $t(v) = \frac{1}{10 \times 10^{-3}} v$.

3.7 Hardware-software integration tests

By means of the same procedures presented in Section 3.6, validation data sets were obtained. For the adjustment of the Shunt curve, a maximum error of 4% was found; for the load cell curve a maximum error of 9% was found; and for the LVDT curve, a maximum error of 4.5% was found.

3.8 System integration

In this phase, the whole system was integrated. A dynamic experiment code was generated. Such experiment is divided into two parts: (i) isotonic test, in which the load is held constant and the displacement is measured, and (ii) isometric test, in which the actuator length is held constant and the contraction force due to the heating is measured. The electric current and temperature are also measured.

3.9 Experimental test platform

The experimental platform is presented in Figure 9. A photograph of the platform is shown in Figure 10.

In the isotonic test, the higher end of the actuator is connected to the load cell and the lower end is connected a trail (with a 150 g weight) which is

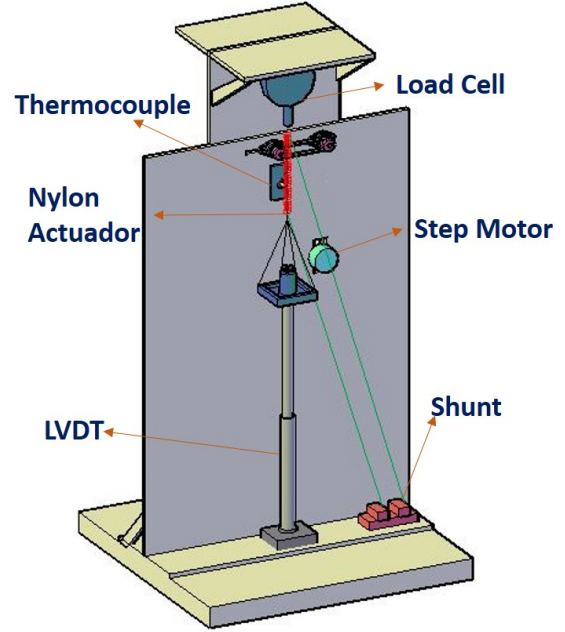


Figure 9: Experimental test platform.

fixed to the LVDT mobile stem. When the actuator is contracting, it pulls the LVDT stem and the displacement is measured. The LVDT body was installed on the platform in a way that stem would not cause any friction due to the actuator contraction and distension. In the isometric test, the LVDT stem is held completely raised and fixed, in a way that, during the heating, the actuator cannot contract, and the force with which it actuates is measured.

3.10 Actuator manufacturing

To obtain a nylon actuator, we have applied the process of coiling induced by twisting the precursor fiber (untwisted nylon fiber), described by Cherubini et al. (2015). The 500 mm length precursor fiber was a monofilament of 0.4 mm diameter nylon.

This process consists of fixing the higher end of the fiber to a rotary motor axis and fixing the lower end to a weight of 100 g, that keeps the fiber tensioned. The lower end is fixed to prevent the rotation around the vertical axis. This way, each turn of the motor axis adds up one turn of the fiber torsion. The weight is free to slide up and down. As the motor rotates at a speed of approximately 600 rpm, the fiber is twisted and shrinks in length. When the torsion is above the critical torsion density, the coiling process starts spontaneously, and the nylon assumes a spring shape. By the end of the process, the actuator obtained is 90 mm in length and 1 mm in diameter.

After the actuator manufacturing process, it is necessary to perform a cyclic thermal training of heating and cooling to ensure a reversible and stable thermal actuation with minimum hysteresis

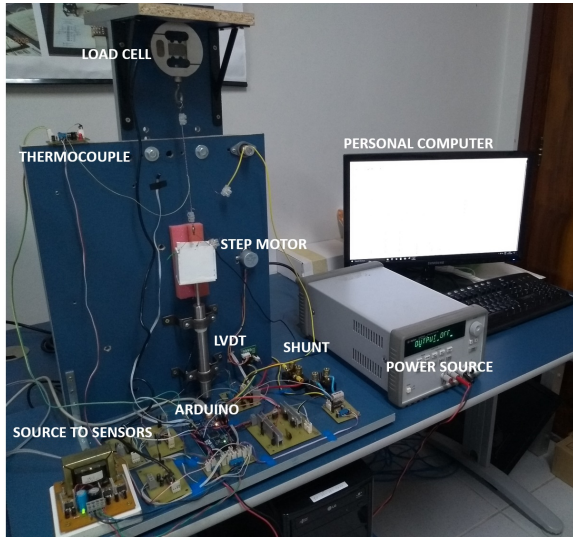


Figure 10: Photograph of the platform.

(Sharafi and Li, 2015). The procedure adopted is similar to the static experiment, in which the actuator is heated by Joule effect caused by the electric current in the 0.8 mm diameter copper wire. The actuator was heated up to 160 °C, that was the maximum temperature the actuator could withstand without damage, and cooled naturally by convection down to room temperature (about 25 °C). The steady state was reached after six cycles and the actuator final length was 120 mm.

4 Results and discussion

For characterizing the nylon actuator, of 1 mm diameter and 120 mm in length obtained from the procedure presented in Section 3.10, we have performed the whole system integration test, which consisted in the performing the dynamic experiment.

4.1 Acceptance tests

The responses of temperature, force, and displacement to the electric current input signal are presented in Figure 11. Such input signal is controlled by a PWM signal, whose duty cycle varies from 10% to 100%, at steps of 10%. In this experiment, both the heating and cooling time intervals were of 50 s.

As shown in Figure 11, the input signal generated a current of up to 6.6 A, heating up the actuator from 26 °C (room temperature) up to 156.4 °C, which generated a force from 1.63 N (before actuator triggering) up to 2.36 N, and reached a 15.2 mm displacement, that is the equivalent to a 12.67% contraction of the 120 mm initial actuator length. The actuator response has a time constant of 4 s from the input signal variation.

The plots of force \times temperature for 40%, 60%, 80%, and 100% duty cycle are shown in Fig-

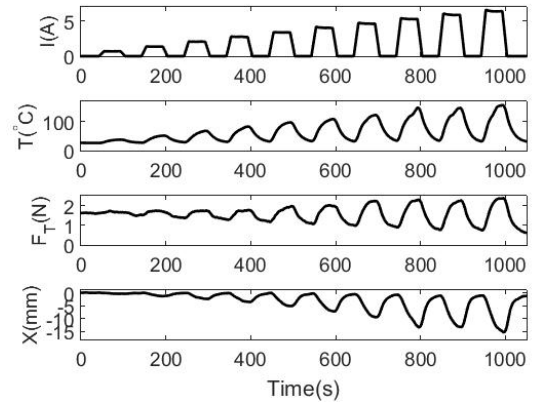


Figure 11: Results of the dynamic test experiment.

ure 12. These are the actuation force versus temperature profiles of the actuator.

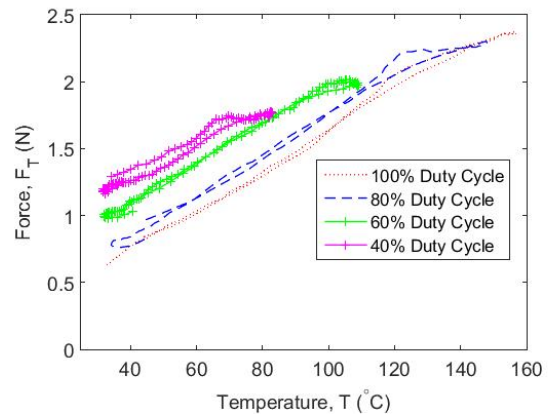


Figure 12: Force \times temperature profile for the nylon actuator.

As shown in Figure 12, the relationship between force and temperature has almost no hysteresis at all operating points. It is also possible to conclude that the curves slopes, that can be approximated by a straight line, are similar, indicating that the expression in (2) is acceptable.

The curves of displacement \times temperature are shown in Figure 13, for 40%, 60%, 80%, and 100% duty cycles.

5 Conclusion and future work

This work presented the design, implementation and tests of an experimental platform to obtain electro thermomechanical responses of an actuator based on a nylon thread. The Model-Based Design Methodology with automatic code generation allowed greater productivity and avoided engineering rework, because imposes verification and tests along all the project phases.

By means of an isotonic test, we have demonstrated that a 120 mm in length and 1 mm diam-

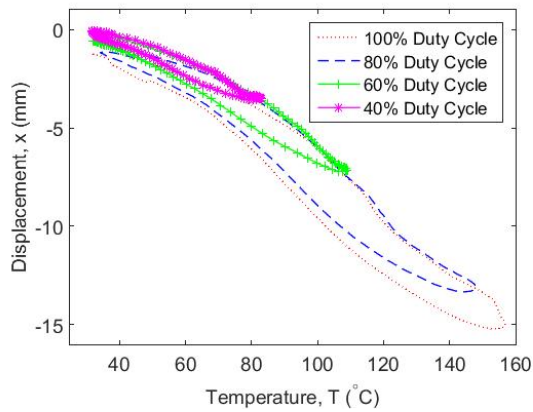


Figure 13: Displacement \times temperature plot.

eter actuator may lift a load of 150 g, contracting up to 15.2 mm (12.67%) when submitted to a temperature of 156.4 °C in response to an electric current as an input signal of average value of 6.6 A that flows through a 0.8 mm diameter copper wire which surrounds the actuator. For the same conditions of electric current and temperature, by means of an isometric test, we have demonstrated the actuator capacity of generating a force of up to 2.36 N.

The force generated by the actuator when heated has a linear relationship with the temperature, while the displacement has an hysteretic response.

In future works, using the data acquired in this work, the parameters of the actuator model will be estimated, whose input is the electric current and output are temperature, force and displacement, in order to demonstrate the validity of the models proposed in 3 and 6. Furthermore, a control system position will be designed and tested.

Acknowledgments

The authors would like to thank the PPgEE-COPELE and CAPES for the necessary support during this work.

References

Aarenstrup, R. (2015). Managing model-based design, *CreateSpace Independent Publishing Platform*.

Arakawa, T., Takagi, K., Tahara, K. and Asaka, K. (2016). Position control of fishing line artificial muscles (coiled polymer actuators) from nylon thread, *Conf. Rec. SPIE/EAPAD'2016*, Vol. 9798, p. 97982W.

Cherubini, A., Moretti, G., Vertechy, R. and Fontana, M. (2015). Experimental character-

ization of thermally-activated artificial muscles based on coiled nylon fishing lines, *AIP Advances* **5**(6): 067158.

Cho, K. H., Song, M.-G., Jung, H., Yang, S. Y., Moon, H., Koo, J. C., Nam, J.-d. and Choi, H. R. (2016). Fabrication and modeling of temperature-controllable artificial muscle actuator, *Conf. Rec. IEEE/BioRob'2016*, pp. 94–98.

Haines, C. S., Lima, M. D., Li, N., Spinks, G. M., Foroughi, J., Madden, J. D., Kim, S. H., Fang, S., de Andrade, M. J., Göktepe, F., Göktepe, Ö., Mirvakili, S., Naficy, S., Lepró, X., Oh, J., Kozlov, M., Kim, S., Xu, X., Swedlove, B., Wallace, G. and Baughman, R. (2014). Artificial muscles from fishing line and sewing thread, *Science* **343**(6173): 868–872.

Kianzad, S., Pandit, M., Bahi, A., Ravandi, A. R., Ko, F., Spinks, G. M. and Madden, J. D. (2015). Nylon coil actuator operating temperature range and stiffness, *SPIE Smart Structures and Materials+ Nondestructive Evaluation and Health Monitoring*, International Society for Optics and Photonics, pp. 94301X–94301X.

Mirvakili, S. M., Ravandi, A. R., Hunter, I. W., Haines, C. S., Li, N., Foroughi, J., Naficy, S., Spinks, G. M., Baughman, R. H. and Madden, J. D. (2014). Simple and strong: Twisted silver painted nylon artificial muscle actuated by joule heating, *Conf. Rec. SPIE/EAPAD'2016*, Vol. 9056, p. 90560I.

Moretti, G., Cherubini, A., Vertechy, R. and Fontana, M. (2015). Experimental characterization of a new class of polymeric-wire coiled transducers, *Conf. Rec. SPIE/BMMMC'2015*, Vol. 9432, p. 94320P.

Seelecke, S. and Muller, I. (2004). Shape memory alloy actuators in smart structures: Modeling and simulation, *Applied Mechanics Reviews* **57**(1): 23–46.

Sharafi, S. and Li, G. (2015). A multiscale approach for modeling actuation response of polymeric artificial muscles, *Soft matter* **11**(19): 3833–3843.

Sutton, L., Moein, H., Rafiee, A., Madden, J. D. and Menon, C. (2016). Design of an assistive wrist orthosis using conductive nylon actuators, *Conf. Rec. IEEE/BioRob'2016*, pp. 1074–1079.

Yip, M. C. and Niemeyer, G. (2015). High-performance robotic muscles from conductive nylon sewing thread, *Conf. Rec. IEEE/ICRA'2015*, pp. 2313–2318.